Environmental Science Advances

ROYAL SOCIETY OF CHEMISTRY

COMMUNICATION

View Article Online
View Journal | View Issue

Cite this: *Environ. Sci.: Adv.*, 2022, **1**, 438

Received 22nd February 2022
Accepted 30th June 2022

DOI: 10.1039/d2va00034b

rsc.li/esadvances

Room-temperature coupling of methane with singlet oxygen†

Anhua Huang,‡[a] Jingsheng Wang,‡[a] Xingyang Wu,[ab] Hangchen Liu,[a] Jun Cai,[a] Guo Qin Xu[c] and Song Ling Wang*[ab]

Owing to emission of methane (CH_4) causing global warming and waste of resources, conversion of CH_4 to value-added chemicals can mitigate environmental sustainability and energy concerns. Direct room-temperature coupling of CH_4 to form ethane (CH_3CH_3) challenges chemists owing to the strong C–H bonds requiring high temperature (>700 °C) for dehydrogenation of CH_4. Oxidative coupling is a promising approach for CH_4 conversion to C_2H_6 using solar energy at room temperature. To achieve high efficiency of C_2H_6 formation, using an appropriate oxidant is a potential strategy to avoid overoxidation during the CH_4 coupling process. Singlet oxygen ($^1O_2$) has typically manifested a mild redox capacity with a high selectivity to attack organic substrate CH_4. Here, we report a synergistic photocatalytic-oxidative route for direct CH_4 coupling. Under solar light irradiation, a high CH_3CH_3 generation rate of 647 μmol g^{-1} h^{-1} is achieved at 25 °C. Our work demonstrates that the solar-oxidative route can result in new and useful C1-based catalytic behaviors.

Environmental significance

Owing to emission of methane (CH_4) causing global warming and waste of resources, conversion of CH_4 to value-added chemicals can mitigate environmental and energy concerns. Direct room-temperature coupling of CH_4 to form ethane (CH_3CH_3) challenges chemists owing to the strong C–H bonds requiring high temperature (>700 °C) for dehydrogenation of CH_4. Oxidative coupling is a promising approach for CH_4 conversion to C_2H_6 using solar energy at room temperature. To achieve high efficiency of C_2H_6 formation, using an appropriate oxidant is a potential strategy to avoid overoxidation during the CH_4 coupling process. Singlet oxygen ($^1O_2$) has typically manifested a mild redox capacity with a high selectivity to attack organic substrate CH_4. Here, we report a synergistic photocatalytic-oxidative route for direct CH_4 coupling. Under solar light irradiation, a high CH_3CH_3 generation rate of 647 μmol g^{-1} h^{-1} is achieved at 25 °C. Our work demonstrates that the solar-oxidative route can result in new and useful C1-based catalytic behaviors.

Taking into account the environmental pollution and global warming caused by the use of traditional fossil energy and the shortage of its reserves, increasing the use of natural gas mainly composed of methane (CH_4) is an inevitable trend,[1] since methane has the advantage of being abundant and relatively inexpensive and clean. However, methane itself is also a greenhouse gas whose greenhouse effect is about 25 times that of carbon dioxide of the same mass.[2] Thus, methane emissions contribute to global warming. On the other hand, the direct use of natural gas as a fuel will also cause environmental pollution and waste of resources, since methane storage and transportation are difficult and it is prone to leakage. These factors have made scientists invest a lot of energy in the research and development of simple and feasible technologies for converting methane into value-added chemical raw materials.

However, a high temperature (>700 °C) is required for thermodynamic dehydrogenation of CH_4 due to the strong C–H bonds (434 kJ mol^{-1}), leading to energy consumption and low selectivity of CH_4 conversion.[3] Photocatalytic methane conversion is a safe, low-energy and environmentally friendly strategy for the direct conversion of methane, since the dissociation of methane at room temperature can be achieved by means of photocatalytic methods using the light energy of sunlight and a suitable photocatalyst. Photocatalytic oxidation is also a promising approach for coupling of CH_4 to form C_2H_6 using solar energy at room temperature.[4] Nevertheless, the major challenge of CH_4 coupling *via* the photocatalytic route is insufficient yield of target CH_3CH_3 and large production of by-products, *e.g.*, HCOOH, CO, and CO_2. Furthermore, noble metal co-catalysts, such as Au, Pd, and Pt, were generally used for promoting the efficiency of coupling of CH_4.[5] Developing oxidative-coupling and noble-metal-free catalyst systems, thus,

[a]*School of Environmental Science and Engineering, School of Chemistry and Chemical Engineering, Shanghai Jiao Tong University, 800 Dongchuan Road, 200240 Shanghai, China. E-mail: wangsl@sjtu.edu.cn*

[b]*China-UK Low Carbon College, Shanghai Jiao Tong University, Shanghai 200240, China*

[c]*Department of Chemistry, National University of Singapore, 117543, Singapore*

† Electronic supplementary information (ESI) available. See https://doi.org/10.1039/d2va00034b

‡ These authors contributed equally to this work.

is highly desirable for photocatalytic CH_4 coupling at room temperature.

Traditionally, chemical oxidants, including O_2, H_2O_2, and CO_2, have been proven to be important in oxidative activation of CH_4 to hydrocarbons, such as methanol.[6] Actually, these oxidants potentially generate reactive oxygen species (ROS), such as the superoxide radical anion ($O_2^{\bullet-}$), hydroxyl radical ($^{\bullet}OH$), sulfate radical ($SO_4^{\bullet-}$) and singlet oxygen ($^1O_2$), which are crucial in activation of CH_4.[7] In particular, the $^1O_2$-based system typically manifested a mild redox capacity (2.2 V) with a high selectivity to attack organic substrates, compared to other free radicals such as $SO_4^{\bullet-}$ (2.5–3.1 V) and $^{\bullet}OH$ (2.7 V) (see Fig. 1).[8]

Peroxymonosulfate (P) as an excellent alternative oxidant has been confirmed to be the main source of HSO_5^- which can produce $^1O_2$, $^{\bullet}OH$, and $SO_4^{\bullet-}$ radicals.[9] In particular, P can be utilized for selective oxidation of organic substances during which $^1O_2$ is generated and serves as a mild oxidant with distinct reactivity towards different substrates.[10] Importantly, the HSO_5^- molecule has a higher oxidizing potential (1.82 V) than H_2O_2 (1.76 V), and is thus more promising for activation of CH_4.[7] Therefore, P is often applied as an electron acceptor in photocatalytic degradation of organic pollutants.[11] Nevertheless, P has never been studied for selective activation of CH_4.

Herein, we develop a TiO_2–$^1O_2$ system for the photocatalytic-oxidative route for CH_4 coupling to form CH_3CH_3 with solar light at room temperature. Other oxidants, including O_2, H_2O_2, and CO_2, have been investigated to illustrate the important role of HSO_5^- in selectively controlling the coupling of CH_4 to form C_2H_6. Further, an $^1O_2$ involving radical-mediated pathway is proposed to explain the high activity of C_2H_6 formation from CH_4. This work provides an alternative new approach for effective coupling of CH_4 to form C_2H_6 at room temperature.

The XRD patterns of TiO_2 in Fig. S1a† show the typical anatase and rutile diffraction peaks. The particle morphology with the size range of 10–30 nm and crystalline structure have been clearly indicated by the TEM and HRTEM images of TiO_2, respectively (Fig. S1b and c†). Fig. 1 shows the band structure of TiO_2 and the redox potentials of $H_2O_2/^{\bullet}OH$, $H_2O/^{\bullet}OH$, $O_2/O_2^{\bullet-}$, $^1O_2/O_2^{\bullet-}$, $SO_5^{\bullet-}/HSO_5^-$, and $HSO_5^-/SO_4^{\bullet-}$.[12,13] Based on these band and redox positions, the TiO_2 material is expected to present enhanced performance for radical generation and activation of CH_4.

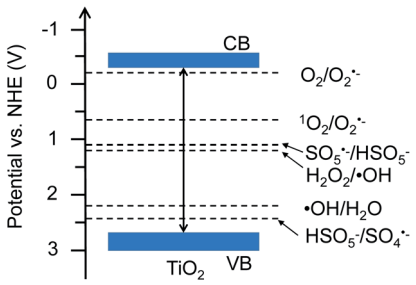

Fig. 1 Band structure of TiO_2 (Degussa P25) and redox potentials of reactive oxygen species.

In order to reveal the photocatalytic performance of the TiO_2–$^1O_2$ system, we first made a comparison of control experiments based on different reaction conditions, including light, catalyst, and HSO_5^- (see Fig. 2a). Under solar light irradiation, TiO_2 with HSO_5^- as oxidant gave rise to an excellent performance for selective generation of C_2H_6, with a rate of 647 μmol g^{-1} h^{-1}, much higher than the 180 and 89 μmol g^{-1} h^{-1} for the two by-products CH_3OH and HCOOH, respectively, leading to a calculated C_2H_6 selectivity up to 75%. Notably, HSO_5^- can be independently activated by solar light with the corresponding reaction: $HSO_5^- \rightarrow SO_4^{\bullet-} + {}^{\bullet}OH$.[14] The $^{\bullet}OH$ radical enables activation of CH_4 to produce $^{\bullet}CH_3$ species which are essential for C_2H_6 and CH_3OH generation. Under these conditions only a little C_2H_6, CH_3OH, HCOOH, and CO were detected, as displayed in Fig. 2a. For TiO_2 as catalyst, the photo-generated carriers reacting with HSO_5^- generate more $^1O_2$ which activates CH_4 to generate $^{\bullet}CH_3$ species, thus accelerating the coupling of $^{\bullet}CH_3$ to form C_2H_6.

To reveal the crucial role of $^1O_2$ in selective conversion of CH_4 to C_2H_6, a control experiment was conducted using different oxidants for the conversion of CH_4. Fig. 2b summarizes the results of CH_4 oxidation with various oxidants ($^1O_2$, H_2O_2, O_2, and CO_2) under solar light irradiation. Apart from a little bit of CH_3OH, trace amounts of C_2H_6 were found for H_2O_2, O_2, and CO_2 as oxidants, as shown in Fig. 2b. In contrast, the reaction with $^1O_2$ as oxidant remarkably promotes the conversion of CH_4 and selective generation of C_2H_6. Therefore, we conclude that $^1O_2$ possesses superiority in view of the photocatalytic activity and selectivity for C_2H_6 generation. This is probably attributed to the specific band structure of TiO_2 and more positive redox potential of $HSO_5^-/SO_4^{\bullet-}$, thus favouring

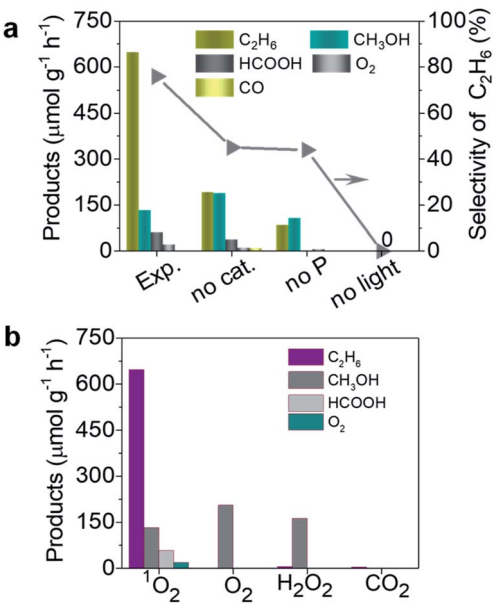

Fig. 2 Photocatalytic performance of the TiO_2–$^1O_2$ system under solar light irradiation: (a) comparison of this work (Exp.) and control experiments by varying conditions (no light, no P, and no cat.); (b) products obtained with different oxidants ($^1O_2$, O_2, H_2O_2, and CO_2).

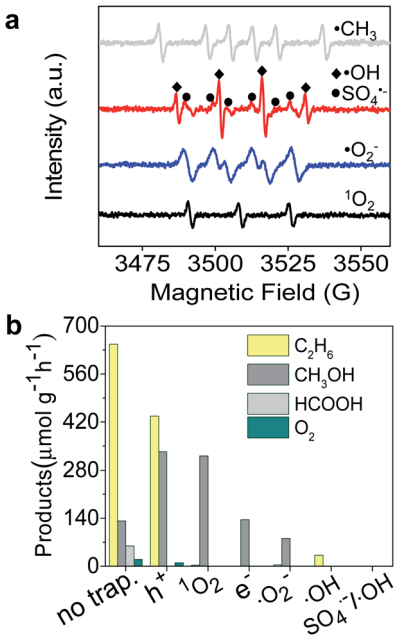

Fig. 3 (a) ESR spectra of $^{\bullet}CH_3$, $^{\bullet}OH$, $SO_4^{\bullet-}$, and $^{\bullet}O^{2-}$ radicals produced after photocatalytic reaction for 10 min. (b) Products of CH_4 conversion after adding scavengers *para*-quinone, $K_2Cr_2O_7$, $Na_2C_2O_4$, and salicylic acid in the reaction system for trapping $^{\bullet}O^{2-}$, e^-, h^+, and $^{\bullet}OH$, respectively.

generation of $^1O_2$, as shown in Fig. 1. Additionally, to further understand the ability of $^1O_2$, we controlled the amount of P which is the source of $^1O_2$ (Fig. S2a†). As the amount of P was increased from 0 to 0.10 mmol, more C_2H_6 was selectively produced in addition to two other products CH_3OH and HCOOH. Meanwhile, much more over-oxidation by-products (HCOOH, CO, and CO_2) were generated as it increased to 0.4 mmol, as displayed in Fig. 3a and b. This is presumably owing to the over-oxidation of CH_4. It is possible that excessive P may undergo a photoreaction ($HSO_5^- \rightarrow SO_4^{\bullet-} + {}^{\bullet}OH$) and produce $^{\bullet}OH$, leading to the formation of CH_3OH and subsequent over-oxidization to HCOOH.

Therefore, excessive P normally results in formation of other by-products, leading to less C_2H_6. This result further suggests that an appropriate amount of P contributes to selective conversion of CH_4 to C_2H_6. Importantly, such a noble-metal free catalyst system presents remarkable coupling of CH_4 to form CH_3CH_3 compared to the various reported noble metal-based catalysts (see Table 1).

To gain a better understanding of the mechanism of the photocatalytic process for selective conversion of CH_4 to C_2H_6, we used electron spin resonance (ESR) characterization and performed trapping experiments of active species, where 5-dimethyl-1-pyrroline-*N*-oxide (DMPO) was used as a trapping reagent to detect $^{\bullet}CH_3$, $SO_4^{\bullet-}$, $^{\bullet}OH$, and $O_2^{\bullet-}$ species. 2,2,6,6-Tetramethylpiperidine (TEMP) was used for detection of $^1O_2$. As shown in Fig. 3a, the typical $^{\bullet}CH_3$, $SO_4^{\bullet-}$, $^{\bullet}OH$, $O_2^{\bullet-}$, and $^1O_2$ radical species were obviously formed during the photocatalytic process. To verify the distinctive roles of these species in selective conversion of CH_4, we carried out trapping experiments using the corresponding scavengers, as displayed in Fig. 2a. The detailed reactions between scavenger reagents and active species are described in the ESI.† In Fig. 3b, the generation of C_2H_6 was significantly suppressed after trapping the $^1O_2$ in Fig. 2b, while CH_3OH production was slightly promoted during this process. This result suggests that $^1O_2$ remarkably facilitates the formation of C_2H_6 and the $^{\bullet}OH$ radical prefers to activate CH_4 for generation of CH_3OH. However, a fraction of C_2H_6 was still detectable even after trapping $^{\bullet}OH$ in the reactive system, which is probably attributed to the remaining $^1O_2$ radicals. Apart from a certain amount of CH_3OH, C_2H_6 was never found in the absence of $O_2^{\bullet-}$ active species (see Fig. 3b). This indicates that $O_2^{\bullet-}$ also remarkably determined the selective formation of C_2H_6 which is related to the formation of $^1O_2$. The e^- was also essential for the selective conversion as it initiated the $^1O_2$ generation through chain reactions, which was proven by the absence of C_2H_6 in products after elimination of photogenerated electrons. On the other hand, h^+ only partially controlled the formation of C_2H_6 based on an h^+ trapping experiment.

Based on the above experimental analysis, we proposed a plausible mechanism. As displayed in Scheme 1, photo-induced electrons reacted with HSO_5^- and generated $SO_4^{\bullet-}$ and $^{\bullet}OH$ radicals (eqn (1) and (2)).[24] Meanwhile, direct light irradiation accelerated the generation of $SO_4^{\bullet-}$ and $^{\bullet}OH$ radicals (eqn (3)).[7] O_2 was formed based on the reactions described by eqn (4)–(6),[7] which agrees well with the trace amount of O_2

Table 1 Comparison of photocatalytic conversion of CH_4 to CH_3CH_3 over reported noble-metal-based catalysts

Catalysts	Light source	Temperature (°C)	C_2H_6 (μmol g^{-1} h^{-1})	Ref.
6.0 wt% Ag–HPW/TiO_2	Xe lamp 400 W ($200 < \lambda < 1000$ nm)	30	20.3	15
1.0 wt% Pt/HGTS	Xe lamp 300 W	60	0.63	16
11.7 wt% Au/m-ZnO	Xe lamp 300 W (solar light)	30	11.3	17
AuPd/ZnO (Pd, 1.0 wt%)	Xe lamp 300 W (solar light)	30	17.7	18
0.5 wt% Pd/Ga_2O_3	Xe lamp 300 W ($\lambda = 254$ nm)	45	0.28	19
WO_3, H_2O_2 (2 mM)	Mercury-vapor lamp (UVC-visible light)	55	3.40	20
HBEA	Hg lamp 450 W	70	14.3	21
$Cu_{0.1}Pt_{0.5}$/PC-50	LED 40 W ($\lambda = 365$ nm)	40	68.0	22
Au–ZnO/TiO_2	Xenon lamp 300 W ($300 < \lambda < 500$ nm)	26	188	23
TiO_2, $^1O_2$	Xe lamp 300 W (solar light)	25	647	This work

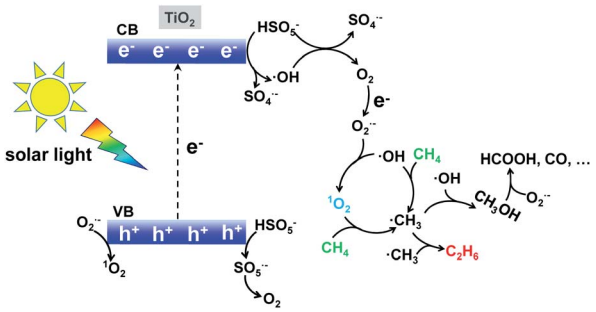

Scheme 1 Singlet oxygen involving radical-pathway mechanism for conversion of methane to ethane with the TiO_2–$^1O_2$ system.

when $^1O_2$ is used as oxidant in Fig. 2b. This O_2 further generated the $O_2^{\cdot-}$ radical according to the reactions described by eqn (7). Consequently, $^1O_2$ was finally produced as a result of the presence of the $O_2^{\cdot-}$ radical (see eqn (8) and (9)).[25] The synthesized $^1O_2$ was able to selectively dehydrogenize CH_4 and generate the $^{\cdot}CH_3$ radical which further underwent coupling, hence producing CH_3CH_3 (eqn (10)–(13)). It is noted that an increasing amount of $^{\cdot}CH_3$ prefers to form C_2H_6,[26] which is competitive with the CH_3OH generation ($^{\cdot}CH_3 + {}^{\cdot}OH \rightarrow CH_3OH$).[27,28] Therefore, when more $^{\cdot}OH$ or $O_2^{\cdot-}$ was present, CH_3OH could be generally produced. This well indicates that the dominant product was CH_3OH when radicals H_2O_2 and O_2 were selected as oxidants in Fig. 2b. Taken together, $^1O_2$ favoured selective production of CH_3CH_3, in comparison with H_2O_2 or O_2-based systems. Apart from the products CH_3CH_3 and CH_3OH, over-oxidation by-products such as HCOOH, CO, and even CO_2 could also be formed (see eqn (14) and (15)) in the presence of the $O_2^{\cdot-}$ radical.[29]

$$HSO_5^- + e^- \rightarrow OH^- + SO_4^{\cdot-} \quad (1)$$

$$HSO_5^- + e^- \rightarrow {}^{\cdot}OH + SO_4^{2-} \quad (2)$$

$$HSO_5^- \rightarrow {}^{\cdot}OH + SO_4^{\cdot-} \quad (3)$$

$$2HSO_5^- + 2{}^{\cdot}OH \rightarrow 2SO_4^{\cdot-} + 2H_2O + O_2 \quad (4)$$

$$HSO_5^- + h^+ \rightarrow H^+ + SO_5^{\cdot-} \quad (5)$$

$$SO_5^{\cdot-} + SO_5^{\cdot-} \rightarrow 2SO_4^{\cdot-} + O_2 \quad (6)$$

$$O_2 + e^- \rightarrow O_2^{\cdot-} \quad (7)$$

$$O_2^{\cdot-} + h^+ \rightarrow {}^1O_2 \quad (8)$$

$$^{\cdot}OH + O_2^{\cdot-} \rightarrow {}^1O_2 + OH^- \quad (9)$$

$$^1O_2 + CH_4 \rightarrow {}^{\cdot}CH_3 \quad (10)$$

$$CH_4 + {}^{\cdot}OH \rightarrow {}^{\cdot}CH_3 + H_2O \quad (11)$$

$$^{\cdot}CH_3 + {}^{\cdot}OH \rightarrow CH_3OH \quad (12)$$

$$^{\cdot}CH_3 + {}^{\cdot}CH_3 \rightarrow C_2H_6 \quad (13)$$

$$CH_3OH + O_2^{\cdot-} \rightarrow HCOOH \quad (14)$$

$$HCOOH + O_2^{\cdot-} \rightarrow CO + CO_2 \quad (15)$$

Conclusions

Solar-light driven selective conversion of methane to ethane has been achieved through a photocatalytic reaction at room temperature. By introducing HSO_5^- into a TiO_2-based photocatalytic system, enhanced yields and selectivity of CH_3CH_3 are obtained largely due to the presence of $^1O_2$ provided by HSO_5^-. Solar light stimulates the TiO_2 catalyst to produce charge carriers (excited electrons and holes) which further activate HSO_5^- to generate $^1O_2$. Detection and trapping experiments of active species further prove that the photocatalytic TiO_2–$^1O_2$ system involves the $^1O_2$ radical pathway mechanism. This report opens up a new possibility for efficient conversion of methane to ethane with solar energy at ambient temperature.

Author contributions

Anhua Huang and Jingsheng Wang prepared the samples, carried out the experiments, analysed the data and prepared the paper; Xingyang Wu and Hangchen Liu assisted with the characterization and photocatalytic tests; Jun Cai and Guo Qin Xu reviewed and edited the manuscript; Song Ling Wang supervised this work and reviewed/edited the manuscript; all authors discussed the results and commented on the manuscript.

Conflicts of interest

There are no conflicts to declare.

Acknowledgements

This work was sponsored by the Shanghai Pujiang Talent Program (No. 19PJ1405200) and the Startup Fund for Youngman Research at SJTU (SFYR at SJTU, No. WF220516003).

Notes and references

1 H. Herzog, B. Eliasson and O. Kaarstad, Capturing greenhouse gases, *Sci. Am.*, 2000, **282**, 72–79.
2 H. Song, X. Meng, Z.-j. Wang, H. Liu and J. Ye, Solar-energy-mediated methane conversion, *Joule*, 2019, **3**, 1606–1636.
3 Y. Zeng, H. C. Liu, J. S. Wang, X. Y. Wu and S. L. Wang, Synergistic photocatalysis–Fenton reaction for selective conversion of methane to methanol at room temperature, *Catal. Sci. Technol.*, 2020, **10**, 2329–2332.
4 L. Yuliati and H. Yoshida, Photocatalytic conversion of methane, *Chem. Soc. Rev.*, 2008, **37**, 1592–1602.
5 L. Yu, Y. Shao and D. Li, Direct combination of hydrogen evolution from water and methane conversion in a photocatalytic system over Pt/TiO_2, *Appl. Catal., B*, 2017, **204**, 216–223.

6 Y. Kang, Z. Li, X. Lv, W. Song, Y. Wei, X. Zhang, J. Liu and Z. Zhao, Active oxygen promoted electrochemical conversion of methane on two-dimensional carbide (MXenes): from stability, reactivity and selectivity, *J. Catal.*, 2020, **393**, 20–29.

7 F. Ghanbari and M. Moradi, Application of peroxymonosulfate and its activation methods for degradation of environmental organic pollutants, *Chem. Eng. J.*, 2017, **310**, 41–62.

8 S. Zhu, X. Li, J. Kang, X. Duan and S. Wang, Nonradical oxidation in persulfate activation by graphene-like nanosheets (GNS): differentiating the contributions of singlet oxygen ($^1O_2$) and sorption-dependent electron transfer, *Environ. Sci. Technol.*, 2019, **53**, 307–315.

9 D. Dai, Z. Yang, Y. Yao, L. Chen, G. Jia and L. Luo, Persulfate activation on crystallographic manganese oxides: mechanism of singlet oxygen evolution for nonradical selective degradation of aqueous contaminants, *Catal. Sci. Technol.*, 2017, **7**, 934–942.

10 Y. Zhou, J. Jiang, Y. Gao, J. Ma, S.-Y. Pang, J. Li, X.-T. Lu and L.-P. Yuan, Activation of peroxymonosulfate by benzoquinone: a novel nonradical oxidation process, *Environ. Sci. Technol.*, 2015, **49**, 12941–12950.

11 M. Ahmadi, F. Ghanbari and M. Moradi, Photocatalysis assisted by peroxymonosulfate and persulfate for benzotriazole degradation: effect of pH on sulfate and hydroxyl radicals, *Water Sci. Technol.*, 2015, **72**, 2095–2102.

12 Y. Shiraishi, Y. Ueda, A. Soramoto, S. Hinokuma and T. Hirai, Photocatalytic hydrogen peroxide splitting on metal-free powders assisted by phosphoric acid as a stabilizer, *Nat. Commun.*, 2020, **11**, 3386.

13 J. Lim, Y. Yang and M. Hoffmann, Activation of Peroxymonosulfate by Oxygen Vacancies-Enriched Cobalt-Doped Black TiO_2 Nanotubes for the Removal of Organic Pollutants, *Environ. Sci. Technol.*, 2019, **53**, 6972–6980.

14 M. G. Antoniou, A. A. de la Cruz and D. D. Dionysiou, Degradation of microcystin-LR using sulfate radicals generated through photolysis, thermolysis and e-transfer mechanisms, *Appl. Catal., B*, 2010, **96**, 290–298.

15 X. Yu, V. L. Zholobenko, S. Moldovan, D. Hu, D. Wu, V. V. Ordomsky and A. Y. Khodakov, Stoichiometric methane conversion to ethane using photochemical looping at ambient temperature, *Nat. Energy*, 2020, **5**, 511–519.

16 S. Wu, X. Tan, J. Lei, H. Chen, L. Wang and J. Zhang, Ga-doped and Pt-loaded porous TiO_2–SiO_2 for photocatalytic nonoxidative coupling of methane, *J. Am. Chem. Soc.*, 2019, **141**, 6592–6600.

17 L. Meng, Z. Chen, Z. Ma, S. He, Y. Hou, H.-H. Li, R. Yuan, X.-H. Huang, X. Wang and X. Wang, Gold plasmon-induced photocatalytic dehydrogenative coupling of methane to ethane on polar oxide surfaces, *Energy Environ. Sci.*, 2018, **11**, 294–298.

18 W. Jiang, J. Low, K. Mao, D. Duan, S. Chen, W. Liu, C.-W. Pao, J. Ma, S. Sang and C. Shu, Pd-Modified ZnO–Au Enabling Alkoxy Intermediates Formation and Dehydrogenation for Photocatalytic Conversion of Methane to Ethylene, *J. Am. Chem. Soc.*, 2020, **143**, 269–278.

19 S. P. Singh, A. Anzai, S. Kawaharasaki, A. Yamamoto and H. Yoshida, Non-oxidative coupling of methane over Pd-loaded gallium oxide photocatalysts in a flow reactor, *Catal. Today*, 2020, **375**, 264–272.

20 K. Villa, S. Murcia-López, T. Andreu and J. R. Morante, Mesoporous WO_3 photocatalyst for the partial oxidation of methane to methanol using electron scavengers, *Appl. Catal., B*, 2015, **163**, 150–155.

21 S. Murcia-López, M. C. Bacariza, K. Villa, J. M. Lopes, C. Henriques, J. R. Morante and T. Andreu, Controlled photocatalytic oxidation of methane to methanol through surface modification of beta zeolites, *ACS Catal.*, 2017, **7**, 2878–2885.

22 X. Li, J. Xie, H. Rao, C. Wang and J. Tang, Platinum-and CuO_x-Decorated TiO_2 Photocatalyst for Oxidative Coupling of Methane to C_2 Hydrocarbons in a Flow Reactor, *Angew. Chem., Int. Ed.*, 2020, **59**, 19702–19707.

23 S. Song, H. Song, L. Li, S. Wang, W. Chu, K. Peng, X. Meng, Q. Wang, B. Deng, Q. Liu, Z. Wang, Y. Weng, H. Hu, H. Lin, T. Kako and J. Ye, A selective Au-ZnO/TiO_2 hybrid photocatalyst for oxidative coupling of methane to ethane with dioxygen, *Nat. Catal.*, 2021, **4**, 1032–1042.

24 X. Chen, W. Wang, H. Xiao, C. Hong, F. Zhu, Y. Yao and Z. Xue, Accelerated TiO_2 photocatalytic degradation of Acid Orange 7 under visible light mediated by peroxymonosulfate, *Chem. Eng. J.*, 2012, **193**, 290–295.

25 X. Li, J. Liu, A. I. Rykov, H. Han, C. Jin, X. Liu and J. Wang, Excellent photo-Fenton catalysts of Fe–Co Prussian blue analogues and their reaction mechanism study, *Appl. Catal., B*, 2015, **179**, 196–205.

26 S. Murcia-López, K. Villa, T. Andreu and J. R. Morante, Partial oxidation of methane to methanol using bismuth-based photocatalysts, *ACS Catal.*, 2014, **4**, 3013–3019.

27 K. Sahel, L. Elsellami, I. Mirali, F. Dappozze, M. Bouhent and C. Guillard, Hydrogen peroxide and photocatalysis, *Appl. Catal., B*, 2016, **188**, 106–112.

28 M. Hayyan, M. A. Hashim and I. M. AlNashef, Superoxide ion: generation and chemical implications, *Chem. Rev.*, 2016, **116**, 3029–3085.

29 J. Xie, R. Jin, A. Li, Y. Bi, Q. Ruan, Y. Deng, Y. Zhang, S. Yao, G. Sankar and D. Ma, J. Highly selective oxidation of methane to methanol at ambient conditions by titanium dioxide-supported iron species, Tang, *Nat. Catal.*, 2018, **1**, 889–896.